# Prion Seeds Distribute throughout the Eyes of Sporadic Creutzfeldt-Jakob Disease Patients

Christina D. Orrù,[a] Katrin Soldau,[b] Christian Cordano,[c] Jorge Llibre-Guerra,[d,e] Ari J. Green,[c] Henry Sanchez,[f] Bradley R. Groveman,[a] Steven D. Edland,[g,h] Jiri G. Safar,[i,j] Jonathan H. Lin,[b] Byron Caughey,[a] Michael D. Geschwind,[e] Christina J. Sigurdson[b,k]

[a]Laboratory of Persistent Viral Diseases, Rocky Mountain Laboratories, National Institute of Allergy and Infectious Diseases (NIAID), National Institutes of Health (NIH), Hamilton, Montana, USA

[b]Department of Pathology, University of California, San Diego, La Jolla, California, USA

[c]Department of Neurology, Multiple Sclerosis Center, University of California, San Francisco (UCSF), San Francisco, California, USA

[d]Cognitive and Behavioral Research Unit, National Institute of Neurology, Havana, Cuba

[e]Department of Neurology, Memory and Aging Center, University of California, San Francisco (UCSF), San Francisco, California, USA

[f]Department of Pathology, University of California, San Francisco (UCSF), San Francisco, California, USA

[g]Department of Family Medicine & Public Health, University of California, San Diego, La Jolla, California, USA

[h]Department of Neurosciences, University of California, San Diego, La Jolla, California, USA

[i]Department of Pathology, Case Western Reserve University, Cleveland, Ohio, USA

[j]Department of Neurology, Case Western Reserve University, Cleveland, Ohio, USA

[k]Department of Pathology, Immunology, and Microbiology, University of California, Davis, Davis, California, USA

**ABSTRACT** Sporadic Creutzfeldt-Jakob disease (sCJD) is the most common prion disease in humans and has been iatrogenically transmitted through corneal graft transplantation. Approximately 40% of sCJD patients develop visual or oculomotor symptoms and may seek ophthalmological consultation. Here we used the highly sensitive real-time quaking-induced conversion (RT-QuIC) assay to measure postmortem prion seeding activities in cornea, lens, ocular fluid, retina, choroid, sclera, optic nerve, and extraocular muscle in the largest series of sCJD patient eyes studied by any assay to date. We detected prion seeding activity in 100% of sCJD eyes, representing three common sCJD subtypes, with levels varying by up to 4 log-fold among individuals. The retina consistently showed the highest seed levels, which in some cases were only slightly lower than brain. Within the retina, prion deposits were detected by immunohistochemistry (IHC) in the retinal outer plexiform layer in most sCJD cases, and in some eyes the inner plexiform layer, consistent with synaptic prion deposition. Prions were not detected by IHC in any other eye region. With RT-QuIC, prion seed levels generally declined in eye tissues with increased distance from the brain, and yet all corneas had prion seeds detectable. Prion seeds were also present in the optic nerve, extraocular muscle, choroid, lens, vitreous, and sclera. Collectively, these results reveal that sCJD patients accumulate prion seeds throughout the eye, indicating the potential diagnostic utility as well as a possible biohazard.

**IMPORTANCE** Cases of iatrogenic prion disease have been reported from corneal transplants, yet the distribution and levels of prions throughout the eye remain unknown. This study probes the occurrence, level, and distribution of prions in the eyes of patients with sporadic Creutzfeldt-Jakob disease (sCJD). We tested the largest series of prion-infected eyes reported to date using an ultrasensitive technique to establish the prion seed levels in eight regions of the eye. All 11 cases had detectable prion seeds in the eye, and in some cases, the seed levels in the retina ap-

proached those in brain. In most cases, prion deposits could also be seen by immu-nohistochemical staining of retinal tissue; other ocular tissues were negative. Our results have implications for estimating the risk for iatrogenic transmission of sCJD as well as for the development of antemortem diagnostic tests for prion diseases.

**KEYWORDS** Creutzfeldt-Jakob disease, RT-QuIC, eye, prion

Prion diseases are rapidly progressive neurodegenerative disorders with no available treatment (1–3). Creutzfeldt-Jakob disease is the most common prion disease in humans, and is classified as sporadic, familial, or iatrogenic (4). Sporadic Creutzfeldt-Jakob disease (sCJD) has been transmitted iatrogenically from prion-contaminated corneal grafts, dura mater transplants, human cadaveric growth hormone, and neuro-surgical instruments (5–9). Although the underlying factors that initiate sCJD are unclear, the cause of prion disease is PrP$^{Sc}$, an infectious misfolded and aggregated form of the cellular prion protein, PrP$^C$ (10, 11). PrP$^C$ is expressed ubiquitously with the highest levels in neural tissues, including retina, although PrP$^C$ expression is higher in brain than retina (12–15).

sCJD is often challenging to diagnose, in part due to the clinical and pathological heterogeneity in the disease phenotype (16–21). The disease is markedly influenced by the *PRNP* prion gene sequence at polymorphic codon 129 (methionine/valine) and by the PrP$^{Sc}$ conformation, which is type 1 or type 2 depending on the protease-resistant aggregate core size (22, 23). sCJD has been divided into six phenotypic variants, or subtypes, that differ by clinical presentation, rate of decline, and pathological targets in the brain and are known as subtype MM1/MV1, VV2, MV2, MM2-cortical, MM2-thalamic, or VV1 (23–25). Approximately one-third of cases have both type 1 and type 2 PrP$^{Sc}$ (MM1/2, MV1/2, and VV1/2) (23).

Visual disturbances are a common early presenting symptom of sCJD (approxi-mately 10 to 20% of cases) often associated with the MM1/MV1 subtype (26, 27), and can include diplopia, supranuclear palsies, and loss of vision (26, 28, 29). Throughout the disease course, more than 40% of cases have visual or oculomotor symptoms (26). In a limited number of reports, the electroretinogram sometimes shows a significant decrease in the β-wave, potentially due to abnormalities in the outer plexiform layer where PrP$^{Sc}$ has been detected (30, 31). By late-stage disease, blindness develops in 25 to 42% of sCJD patients (26, 28), possibly from spongiform degeneration, neuronal loss, and PrP$^{Sc}$ deposits in the thalamus (lateral geniculate) or primary visual cortex.

In addition to the CNS lesions that develop within the visual circuitry, prions have also been directly detected in ocular tissues from a small number of cases, prior to the development of RT-QuIC. In two studies of variant CJD (vCJD), caused by the transmis-sion of bovine spongiform encephalopathy (BSE) to humans, PrP$^{Sc}$ was readily detected in the retina and optic nerve but not in the cornea, lens, vitreous fluid, or sclera by Western blot or immunohistochemical labeling (15, 19). For sCJD, the few reports describing prion detection in the eye show different results, potentially due to the sensitivity of the technique used. PrP$^{Sc}$ was observed in the retina of two patients by immunohistochemical labeling and Western blot (subtypes VV2 and MM1) (15, 32), but not in a third patient studied by a highly sensitive Western blot assay (19). Notably, these studies were conducted prior to the development of the highly sensitive RT-QuIC technique.

As the distribution and extent to which prions are established in the eyes of sCJD patients remain unclear, the risk of iatrogenic prion transmission through ophthalmic procedures is unknown (33, 34). For example, corneal transplantation is an increasingly common surgery, with 185,576 corneal transplantations performed in 116 countries in 2012, more than ever reported previously (35). The United States leads in corneal procurement and transplantation per capita, with approximately 64,000 corneal trans-plants per year (35). Corneal grafts from prion-infected patients have led to two probable and three possible cases of iatrogenic prion transmission, and prion infectivity has been reported from human cornea inoculated into mice (36). The first reported case

**TABLE 1** Patient demographic data and clinical features

| Patient no. | Age of onset (yr) | Disease duration (mo) | Gender | PRNP genotype at codon 129 | sCJD subtype | Clinical signs at onset | Visual symptoms[a] | Visuospatial dysfunction[b] |
|---|---|---|---|---|---|---|---|---|
| 1 | 60 | 1.5 | M | MM | 1 | Cognitive/visual | Yes | No |
| 2 | 60 | 20 | M | MV | 1-2 | Visuospatial | Yes | Yes |
| 3 | 69 | 15 | M | MV | 2 | Behavior/memory | No | No |
| 4 | 79 | 27 | M | MV | 2 | Cognitive | No | No |
| 5 | 55 | 6 | F | VV | 2 | Apraxia | Yes | No |
| 6 | 56 | 10 | F | MM | 1-2 | Language | No | No |
| 7 | 57 | 4 | F | MM | 1 | Motor | No | No |
| 8 | 55 | 24 | F | MV | 1-2 | Behavior | No | No |
| 9 | 63 | 2 | F | MM | 1 | Language | No | Yes |
| 10 | 69 | 6 | F | MV | 1 | Behavior/memory | No | No |
| 11 | 69 | 10 | F | MM | 1-2 | Cognitive/apraxia | No | Yes |

[a]Visual symptoms noted at first through last UCSF visit.
[b]Visuospatial dysfunction based on neuropsychological testing or neurological examination.

of a corneal graft transmission of sCJD occurred in 1974, with death in the recipient 27 months after transplantation. In this case, the diagnosis of CJD was confirmed at autopsy in the donor and recipient (37). Another probable transmission occurred in a 45-year-old woman who developed sCJD after receiving a corneal transplant 30 years earlier from a donor who died from subacute spongiform encephalopathy (38). Three additional cases developed sCJD after corneal transplantation, with the diagnosis confirmed at autopsy in the recipients, but with an incomplete history on the donors (39–41). These reports of iatrogenic prion spread prompted us to investigate the frequency and level of prions in the eyes of sCJD patients to better understand the transmission risk as well as the potential for diagnostic assay development.

Highly sensitive and specific biochemical assays have revolutionized PrP$^{Sc}$ detection and now enable the measurement of minute levels of PrP$^{Sc}$ (attograms to femtograms) from tissues and body fluids, including nasal brushings and CSF (42, 43). The real-time quaking-induced conversion assay (RT-QuIC) detects the misfolding of recombinant monomeric prion protein by prion aggregates or "seeds" within a prion-infected sample (44, 45). Application of RT-QuIC assays to the antemortem diagnosis of sCJD using CSF and nasal brushings has allowed provisional diagnostic sensitivities and specificities approaching 100% (42, 43). Using this extraordinarily sensitive detection method, we investigated the level and distribution of prion seeding activity in the eye tissues of eleven patients who died from sCJD.

## RESULTS

**Clinical features of sCJD patients.** We analyzed the eyes from eleven cases of pathologically confirmed sCJD representing three subtypes as well as six controls having nonprion diseases. All eleven patients were enrolled in the UCSF Memory and Aging Center clinical prion research program in a study approved by the UCSF Committee on Human Research. Participants were evaluated clinically for one or more visits for neurologic deficits as well as for *PRNP* mutations and genotype, and diagnostically by CSF analysis, EEG, and brain MRI. None had mutations in *PRNP* or any history of a known iatrogenic exposure to prions, and the clinical and diagnostic features were consistent with sporadic CJD. At *PRNP* polymorphic codon 129, all three genotypes were represented: MM ($n = 5$), MV ($n = 5$), and VV ($n = 1$).

Three of eleven cases (27%) had visual disturbances such as transient monocular blindness and blurry or double vision (patients 1, 2, and 5), three had impaired visuospatial skills (patients 2, 9, and 11), and no patients had visual field deficits (Table 1). Four of 11 cases had visual signs, including nystagmus, slow ocular pursuit, and increased saccade latency, but these were not considered visual symptoms. Retinal imaging using optical coherence tomography was performed on three sCJD patients (patients 6, 10, and 11) and revealed a modest decrease in peripapillary retinal nerve fiber (pRNFL) layer thickness compared to 20 healthy control eyes (age-balanced
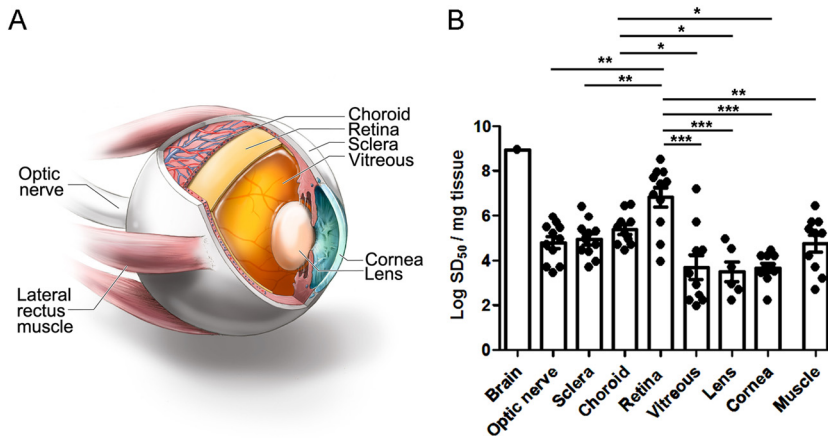
FIG 1 Comparison of prion seed levels in brain (temporal cortex) and ocular compartments from posterior to anterior eye as measured by RT-QuIC analysis. (A) Image showing the ocular tissues tested by RT-QuIC. (B) The seeding dose 50 per mg of tissue ($logSD_{50}$) is shown. The average prion seed level in eye was highest in the retina, and lowest in the vitreous and lens. One vitreous sample, 3 lens samples, and 1 muscle sample were negative and are not shown. Retinal prion seed levels were significantly higher than most other ocular tissues, including optic nerve, sclera, lens, cornea, vitreous, and extraocular muscle. The prion seed level in a representative sCJD brain sample (termporal cortex) is shown for comparison. For retina, optic nerve, sclera, cornea, vitreous, and extraocular muscle, $n = 11$; for choroid, $n = 10$; and for lens, $n = 9$. *, $P < 0.05$; **, $P < 0.01$; ***, $P < 0.001$, one-way ANOVA with Tukey's multiple comparison test. Graphics in panel A by Ryan Kissinger.

reference population) (mean $\pm$ SE: 93.8 $\pm$ 2.2 $\mu$m and 102.0 $\pm$ 2.3 $\mu$m, respectively; $P = 0.07$) (see Fig. S1 in the supplemental material).

Diffusion MRI revealed focal regions of high cortical intensity (cortical ribboning) with restricted diffusion in all cases, with three cases showing cortical ribboning in the occipital (visual) cortex (patients 2, 4, and 11). In addition to cortical involvement, five cases had both striatal and thalamic involvement (patients 2, 3, 6, 8, and 10), three had striatal involvement (patients 4, 7, and 9), and one had thalamic involvement (patient 6). The diagnosis of sCJD was confirmed biochemically by PrP$^{Sc}$ detection in the brain (Fig. S2 and S3).

**PrP$^{Sc}$ levels in six brain regions.** PrP$^{Sc}$ levels in the occipital cortex varied among the patients, with the type 1 cases having higher PrP$^{Sc}$ levels than the type 2 cases (Fig. S2). We also measured PrP$^{Sc}$ by Western blotting samples from six brain regions from each patient, specifically parietal and occipital or frontal cortex, basal ganglia, thalamus, hippocampus, and cerebellum. The PrP$^{Sc}$ levels in each brain region varied within a patient. The thalamus and occipital cortex commonly accumulated high levels of PrP$^{Sc}$, and the cerebellum showed the lowest levels in eight of ten cases examined (Fig. S3).

**Prion seeding activity measured by RT-QuIC.** We next tested the PrP seeding activity by RT-QuIC analysis in eight eye regions, which were extraocular muscle, optic nerve, cornea, lens, vitreous fluid, retina, choroid, and sclera. We found that all eleven sCJD patient eyes were positive for prion seeding activity and showed the highest seeding activity in the retina (Fig. 1). Interestingly, an endpoint dilution assay revealed that seeding activity in eye tissues varied among the patients by up to 4 log-fold (Fig. 1). Prion seed levels in the retina were significantly higher than the extraocular muscles, optic nerve, cornea, lens, vitreous fluid, and sclera (Fig. 1 and 2) ($P < 0.0001$, ANOVA with Tukey's posttest). The lens and vitreous fluid tended to show the lowest seeding activity in most patients and were negative in three patients and one patient, respectively. The high seed levels in the vitreous from two patients may have been due to spread from the retinal layer, as both patients had very high seed levels in the retina. Similarly, the choroid consistently showed high seed levels that were significantly higher than cornea, lens, and vitreous fluid; prion seeds emanating from the retinal layer may have contributed to the high levels. The cornea and extraocular muscle had
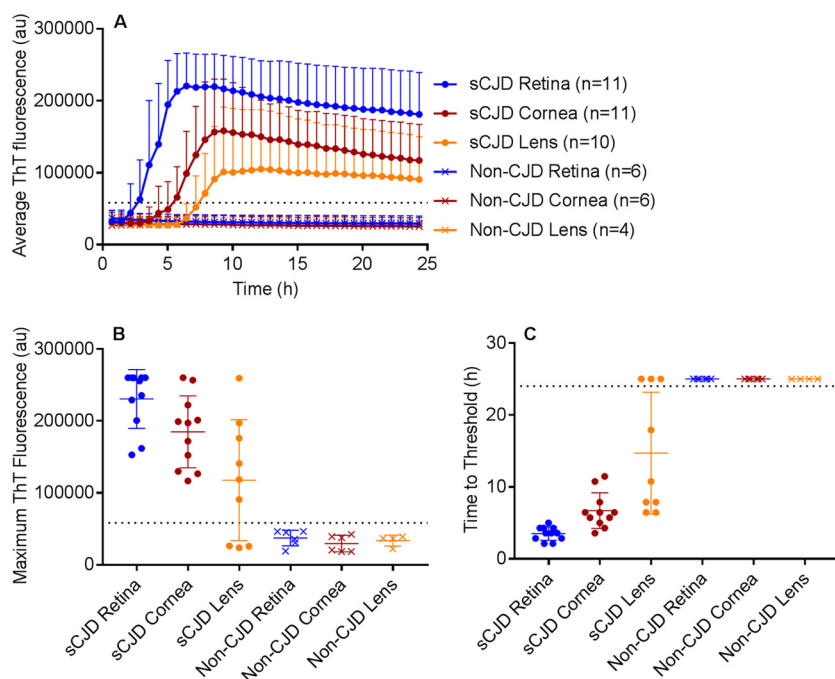
**FIG 2** RT-QuIC of retina, cornea, and lens from sCJD and non-sCJD patients. (A) The average prion seeding amplification kinetics are shown for retina (blue), cornea (red), and lens (orange) from sCJD (circles) and non-CJD (X's) patients. The dotted line indicates the ThT fluorescence threshold for a positive result (see Materials and Methods). (B) The maximum ThT fluorescence reached within 24 hours is shown. The thin lines represent mean and standard deviation, whereas the dotted line indicates the ThT fluorescence threshold for a positive result. (C) The time to reach the threshold for positivity is shown for each sample. The dotted line indicates the end of the 24-hour experiment. If a sample did not reach the threshold within 24 h, it was marked as 25 h to indicate a negative result. $n = 4$ (lens) or 6 (retina, cornea) non-CJD control cases were analyzed.

lower seeding activity relative to the retina (Fig. 1 and 2). None of the six control cases showed seeding activity in any ocular tissue (Fig. 2).

Prion seeding activity in the retina ranged from levels $10^1$-fold to $10^4$-fold lower than sCJD brain (Fig. 1), potentially due to lower PrP$^C$ expression, and higher seeding activity did not correlate with the presence of visual symptoms. We assessed whether the seeding activity in the retina correlated with age, gender, disease duration, *PRNP* genotype, or sCJD subtypes, but found no evidence of a correlation (Fig. S4). A previous report suggested that the sCJD subtype might influence the levels of prion deposits in retina (32). We found that the VV2 subtype showed the highest seed levels in retina, with the MM1-2 and MV1-2 mixtures also tending to show high levels. The MM/MV1 cases instead showed a broad distribution of seeding activity throughout the eye.

**Retinal PrP$^{Sc}$ distribution by immunohistochemistry.** To determine the distribution of prions within the retina, we immunolabeled all eyes for PrP. Nearly all sCJD patients showed PrP$^{Sc}$ deposits in the retina (9 of 11, 82%, of cases) with discrete aggregates visible in the plexiform layers, which consist of dense networks of neuronal synapses. All nine positive retina cases had PrP$^{Sc}$ deposits in the outer plexiform layer, whereas one case (VV2) showed intense staining and also developed strong PrP$^{Sc}$ labeling in the inner plexiform layer (Fig. 3). The other subtypes primarily differed in the staining intensity, but not the stain distribution. Deposits typically appeared as focal oval intensely stained aggregates approximately 4 to 5 $\mu$m in diameter at evenly spaced intervals every 15 to 20 $\mu$m (Fig. 3). The VV2 case also showed fine granular deposits throughout the plexiform layers. No PrP$^{Sc}$ deposits were visible in other (nonretinal) ocular tissues in any case. Neither the non-CJD control eyes (Fig. 3) nor the control IgG isotype-labeled sCJD eyes showed any PrP$^{Sc}$ deposition.
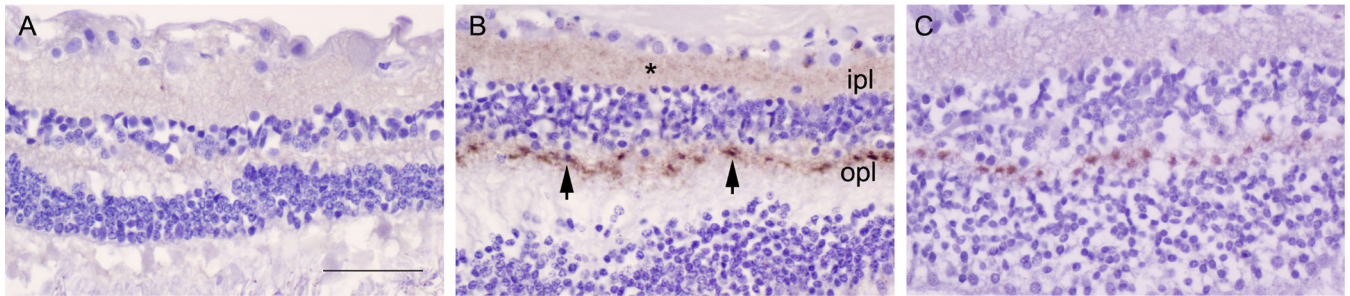
**FIG 3** PrP$^{Sc}$ deposits in retinal plexiform layers. (A) Retina from a non-CJD control patient. (B) Retina from an sCJD patient having abundant labeling of PrP$^{Sc}$ deposits (patient 5, VV2). Deposits consisted of an admixture of diffuse and focal PrP$^{Sc}$ (arrowheads) in the outer plexiform layer (opl) as well as diffuse aggregates (*) in the inner plexiform layer (ipl). (C) Retina from an sCJD patient, subtype MM1 (patient 1), showing PrP$^{Sc}$ in the opl, but not the ipl. Scale bar = 50 $\mu$m.

## DISCUSSION

We detected high prion seed levels in 100% of sCJD patient eyes from three common subtypes and two mixed subtypes, MM1/MV1, VV2, MV2, MM1-2, and MV1-2, using the exceptionally sensitive and quantitative RT-QuIC technique. In more than half the cases, prion seeding activities in retina were remarkably high and approached levels in brain, consistent with efficient prion conversion in neural tissue. The VV2 subtype showed the highest prion seeding activities in the retina and visible deposits in the inner and outer plexiform layers (46). In all other subtypes, retinal prion seeding activities were at least 0.5-log lower; however, prion deposits were consistently visible by IHC in the outer plexiform layer. Ironside and colleagues also reported prion immunolabeling in the plexiform layers from a VV2 patient and an MM1 sCJD patient, with more widespread deposition in the VV2 case as seen here (15, 32). We found that strong prion immunolabeling in the retina correlated with high prion seeding activity.

In all sCJD cases, prion seeding activity accumulated in other (nonretinal) ocular tissues, specifically the choroid, sclera, optic nerve, and cornea, as well as extraocular muscles, lens, and vitreous of most eyes. We noted that high prion seed levels in the optic nerve correlated with high seed levels in the retina, but not in the cornea. Surprisingly, all corneas contained low to moderate prion seeding activity, and levels did not vary substantially among the patients. These differences may reflect prion entry by multiple cranial nerves transporting PrP$^{Sc}$, as prions may be spreading from prion-infected brain into the retina by retrograde axonal transport in the optic nerve (47–50). Prions may be accumulating in the abundant small nerves within the cornea, originating from cranial nerves V and VII.

Our findings support the World Health Organization classification of eye components as having high prion infectivity and have implications for patient safety. As the early-disease phase of sCJD often includes visual symptoms (27–29), patients with sCJD will often have diagnostic assessments performed by an ophthalmologist, potentially contaminating instruments. Experimental models have shown that prions spread from brain to the retina in mice by 60% of the incubation period, prior to the onset of clinical disease (51). Although in humans it is not yet clear when prions accumulate in the eye, the finding of prion seeding activity in all sCJD eyes bolsters recommendations for single-use instruments or other decontamination procedures to prevent iatrogenic prion transmission. Cadaveric corneas have been a source of iatrogenic prion transmission, and grafts are commonly performed (35). With the increased frequency of corneal grafting worldwide, optimizing biosynthetic substitutes would be a justified research priority and is currently under development in multiple laboratories (54, 55).

In all sCJD patient eyes examined, PrP$^{Sc}$ aggregates were highly visible in the posterior retina, an accessible CNS window that could potentially be exploited for the early diagnosis of prion disease. For example, an electroretinogram is an antemortem, noninvasive diagnostic tool that may reveal early electrical abnormalities, particularly considering the prion deposits in synaptic plexi. Because other protein aggregates such

as amyloid-$\beta$, $\alpha$-synuclein, and tau may also spread from brain to retina, it would also be important to continue to evaluate eyes from patients having more common neurodegenerative diseases, such as Alzheimer's disease, synucleinopathies, and tauopathies, particularly in light of recent findings showing the prion-like spread of protein aggregates through the CNS (56–59).

## MATERIALS AND METHODS

**Patients with sporadic Creutzfeldt-Jakob disease and controls.** This prospective study of sCJD patients was initiated in July 2015 and continued through July 2017. Patients were referred to the UC San Francisco (UCSF) Memory and Aging Center for rapidly progressive neurologic disease. All patients had extensive clinical testing, including brain MRI, CSF analysis for 14-3-3, neuron-specific enolase (NSE), and total tau. All were classified as probable sCJD by UCSF clinical and radiological diagnostic criteria (60, 61) and were ruled out for genetic prion disease by PRNP analysis (done through the National Prion Disease Pathology Surveillance Center [NPDPSC], Case Western Reserve University, Cleveland, OH). The mean age of sCJD patients at disease onset was 63 $\pm$ 2 years (mean $\pm$ SE), and consisted of seven women and four men. The duration of clinical neurologic signs ranged from 1.5 to 27 months (mean $\pm$ SD: 11 $\pm$ 9 months). Control cases consisted of five men and one woman and ranged from 51 to 90 years old (mean $\pm$ SD: 70 $\pm$ 14 years). Two of the control cases died of neurodegenerative disease (Alzheimer's disease) and four controls died of nonneurologic disease (neoplasia).

**Study oversight.** This study was approved by the ethics committee at UC San Francisco. Informed consent was received from all patients (IRB Study Number: 10-04905). All ocular and brain tissues examined at UCSD and NIAID were obtained on autopsy; this testing was therefore exempt from review by the NIH Office of Human Subjects Research Protections.

**PRNP genotyping.** The open reading frame of the PRNP gene was sequenced from all patient samples to test for any mutations in the PrP sequence and to determine the genotype at polymorphic codon 129 (methionine or valine; performed at the NPDPSC, Case Western Reserve University, Cleveland, OH). Genomic DNA was extracted from frozen brain tissue samples using Qiagen QIAamp DNA minikit (Qiagen, Gaithersburg, MD) according to the manufacturer's protocol and a 760-bp fragment corresponding to the human PrP gene (residues 5 to 258) was PCR amplified using primers HRM-F (5'-TAT GTGGACTGATGTCGGCCTCTGCAAGAAGCGC-3') and HRM-R (5'-CCACCTCAATTGAAAGGGCTGCAGGTGGA TAC-3') with defined cycling conditions (62, 63). The Met/Val polymorphism at codon 129 and mutation of the PrP gene coding region were determined by deep (63) or direct Sanger sequencing as previously described (22, 62). Nucleotide sequences from both deep and Sanger sequencing were analyzed using DNASTar Lasergene Software Suite v.7.1.0 (Madison, WI). There were no mutations discovered in any of the patients. Patients consisted of 129 MM (5), MV (5), and VV (1).

**Optical coherence tomography.** Antemortem retinal imaging was performed bilaterally using Spectralis spectral-domain OCT (Heidelberg Engineering, Heidelberg, Germany, Eye Explorer software version 1.9.10.0) by two trained technicians under standard ambient conditions (illuminance level of 80 to 100 foot-candles). Peripapillary retinal nerve fiber layer (RNFL) thickness was obtained with a 360° RNFL-B circle scan (100 ART; 1,536 A scan per B scan) located at 3.4 cm from the center of the optic nerve head.

Macular volumetric scans consisting of 19 single horizontal axial B-scans (ART > 9; 1,536 A scan per B scan) were acquired in a 20- by 15-degree raster horizontal scan centered on the fovea. Intraretinal layer segmentation was executed to quantify macular RNFL, ganglion cell layer (GCL), inner nuclear layer (INL), inner plexiform layer (IPL), and outer plexiform layer (OPL) through the Viewing Module 6.0 in a semiautomatic way, with manual correction of software errors. Scans that violated international consensus quality control criteria (OSCAR-IB) were excluded from the analysis (64, 65). We followed the APOSTEL guidelines to report OCT studies (66).

**Brain and ocular tissue collection.** Ocular and brain tissues were collected at autopsy from eleven sCJD patients and six controls. One eye was immediately frozen and the second eye was formalin-fixed. Brain sections were collected from six to nine brain regions and frozen. The formalin-fixed eye tissues were immersed in 98% formic acid for 1 h, and postfixed in formalin prior to paraffin-embedding and sectioning. Frozen eyes were thawed and the following tissue sections were collected for analysis by RT-QuIC using clean sterile blades to avoid contamination among the tissues: extraocular muscle, optic nerve, vitreous fluid, lens, cornea, retina, choroid, and sclera.

**Immunohistochemistry for PrP$^{Sc}$ in the eye.** Four-$\mu$m sections of brain were cut onto positively charged silanized glass slides and stained with hematoxylin and eosin or immunostained using antibodies for PrP (12F10). For PrP staining, sections were deparaffinized and incubated for 5 min in 96% formic acid, then washed in water for 5 min, treated with 5 $\mu$g/ml of proteinase K for 7 min, and washed in water for 5 min. Sections were then placed in citrate buffer (pH 6) and heated in a pressure cooker for 20 min, cooled for 5 min, and rinsed in distilled water. Sections were incubated with anti-PrP 12F10 (Cayman Chemical; 1:200) for 45 min followed by anti-mouse IgG conjugated to biotin (Jackson Immunolabs; 1:250) for 30 min, followed by streptavidin-HRP (Jackson Immunolabs; 1:2,000) for 30 min. Sections were then incubated with DAB reagent (Thermo Fisher Scientific) and counterstained with hematoxylin.

**Western blot for PrP$^{Sc}$ in the brain.** Brain samples were homogenized in phosphate-buffered saline (PBS) (20% brain homogenate final [wt/vol]) using a Beadbeater tissue homogenizer. PrP$^{Sc}$ was concentrated from brain samples by performing sodium phosphotungstic acid (NaPTA) precipitation prior to Western blotting (19). Briefly, 50-$\mu$l aliquots of 10% brain homogenate in an equal volume of 4% sarkosyl in PBS were incubated for 30 min at room temperature, then digested with an endonuclease (Benzonase [Sigma]) and with 100 $\mu$g/ml proteinase K at 37°C for 30 min. After addition of NaPTA, MgCl$_2$, and

protease inhibitors (Complete, Roche), extracts were incubated at 37°C for 30 min and centrifuged at 18,000 × *g* for 30 min at 37°C. Pellets were resuspended in 0.1% sarkosyl in PBS prior to electrophoresis and blotting. Membranes were incubated with monoclonal antibody POM1 (discontinuous epitope at C-terminal domain [67]) followed by incubation with an HRP-conjugated anti-mouse IgG secondary antibody (Jackson Immunolabs). The blots were developed using a chemiluminescent substrate (ECL detection kit, Thermo Scientific) and visualized on a Fuji LAS 4000 imager. Quantification of PrP$^{Sc}$ signal was performed using Multigauge V3 software (Fujifilm).

**PrP$^{Sc}$ subtyping.** sCJD is classified into six main subtypes and three mixed subtypes, depending on the codon 129 polymorphism and the electrophoretic profile of the protease-resistant PrP$^{Sc}$ core fragment size, which is 21 kDa (type 1) or 19 kDa (type 2) (23). We assessed the PK-resistant core size and compared the PrP$^{Sc}$ levels in the occipital cortex among the patients. Three sCJD subtypes were represented, consisting of MM1/MV1 ($n = 4$), MV2 ($n = 2$), and VV2 ($n = 1$), as well as MM1-2 and MV1-2 mixtures ($n = 4$).

**Ocular tissue homogenate preparation for RT-QuIC analysis.** Eye homogenates (10% [wt/vol]) were prepared in PBS containing 2 mM CaCl$_2$ and 0.25% (wt/vol) collagenase A (Roche). Glass homogenization beads (1 mm; Biospec) were added to the sample in homogenization buffer and tissues were homogenized for 1 min using a Beadbeater tissue homogenizer (Biospec). The samples were then incubated at 37°C under shaking conditions overnight, homogenized for 1 min, and centrifuged at 2,000 × *g* for 2 min. The supernatant was transferred to a new tube and stored at −80°C for subsequent analysis.

**RT-QuIC analysis for PrP seeding activity in eye tissues.** The RT-QuIC reaction mix was composed of 10 mM phosphate buffer (pH 7.4), 300 mM NaCl, 0.1 mg/ml recombinant Syrian hamster PrP (residues 90 to 230; rPrP$^{Sen}$; GenBank accession number K02234), 10 $\mu$M thioflavin T (ThT), 1 mM EDTA, and 0.001% SDS. Aliquots of the reaction mix (98 $\mu$l) were loaded into each well of a black 96-well plate with a clear bottom (Nunc) and seeded with 2 $\mu$l of eye tissue homogenates at different dilutions. The plate was sealed (plate sealer film, Nalgene Nunc International) and incubated at 55°C in a BMG FLUOstar Omega plate reader at cycles of 1 min shaking (700 rpm double orbital) and 1 min rest. ThT fluorescence measurements (450 ± 10 nm excitation and 480 ± 10 nm emission; bottom read) were taken every 45 min. ThT fluorescence threshold for a positive result was calculated as the mean of all values from negative eye tissues plus three standard deviations. For quantitation, endpoint dilution assays were performed using Spearman-Kärber analyses to estimate the seeding dose (± SE) giving ThT positivity in 50% of technical replicate wells (SD$_{50}$) (44, 68).

**Statistical analysis.** Data are presented as mean ± SEM unless otherwise indicated with group differences tested using standard parametric methods (one-way ANOVA with Tukey's multiple comparison test). *P* values of less than 0.05 were considered statistically significant.

**Data availability.** The authors will make data fully available and without restriction.

## SUPPLEMENTAL MATERIAL

Supplemental material for this article may be found at https://doi.org/10.1128/mBio.02095-18.

**FIG S1**, TIF file, 2.2 MB.
**FIG S2**, TIF file, 0.6 MB.
**FIG S3**, TIF file, 0.9 MB.
**FIG S4**, TIF file, 0.4 MB.

## REFERENCES

1. Prusiner SB. 1998. Prions. Proc Natl Acad Sci U S A 95:13363–13383. https://doi.org/10.1073/pnas.95.23.13363.

2. DeArmond SJ, Prusiner SB. 1995. Etiology and pathogenesis of prion diseases. Am J Pathol 146:785–811.

3. Collinge J. 2016. Mammalian prions and their wider relevance in neurodegenerative diseases. Nature 539:217–226. https://doi.org/10.1038/nature20415.

4. Takada LT, Geschwind MD. 2013. Prion diseases. Semin Neurol 33: 348–356. https://doi.org/10.1055/s-0033-1359314.

5. Ironside JW, Ritchie DL, Head MW. 2017. Prion diseases. Handb Clin Neurol 145:393–403. https://doi.org/10.1016/B978-0-12-802395-2.00028-6.

6. Brown P, Preece M, Brandel J-P, Sato T, McShane L, Zerr I, Fletcher A, Will RG, Pocchiari M, Cashman NR, d'Aignaux JH, Cervenakova L, Fradkin J, Schonberger LB, Collins SJ. 2000. Iatrogenic Creutzfeldt-Jakob disease at the millennium. Neurology 55:1075–1081. https://doi.org/10.1212/WNL.55.8.1075.

7. Collinge J, Palmer MS, Dryden AJ. 1991. Genetic predisposition to iatrogenic Creutzfeldt-Jakob disease. Lancet 337:1441–1442. https://doi.org/10.1016/0140-6736(91)93128-V.

8. Will RG. 2003. Acquired prion disease: iatrogenic CJD, variant CJD, kuru, p 255–265. In Weissmann C, Aguzzi A, Dormont D, Hunter N (ed), Prions for physicians. Oxford University Press, Oxford, United Kingdom.

9. Hoshi K, Yoshino H, Urata J, Nakamura Y, Yanagawa H, Sato T. 2000. Creutzfeldt-Jakob disease associated with cadaveric dura mater grafts in Japan. Neurology 55:718–721. https://doi.org/10.1212/WNL.55.5.718.

10. Prusiner SB. 1982. Novel proteinaceous infectious particles cause scrapie. Science 216:136–144. https://doi.org/10.1126/science.6801762.

11. Prusiner SB, Scott M, Foster D, Pan KM, Groth D, Mirenda C, Torchia M, Yang SL, Serban D, Carlson GA. 1990. Transgenetic studies implicate interactions between homologous PrP isoforms in scrapie prion replication. Cell 63:673–686. https://doi.org/10.1016/0092-8674(90)90134-Z.

12. Bendheim PE, Brown HR, Rudelli RD, Scala LJ, Goller NL, Wen GY, Kascsak RJ, Cashman NR, Bolton DC. 1992. Nearly ubiquitous tissue distribution of the scrapie agent precursor protein. Neurology 42:149–156. https://doi.org/10.1212/WNL.42.1.149.

13. Fournier JG. 2001. Nonneuronal cellular prion protein. Int Rev Cytol 208:121–160. https://doi.org/10.1016/S0074-7696(01)08003-2.

14. Gong J, Jellali A, Forster V, Mutterer J, Dubus E, Altrock WD, Sahel JA, Rendon A, Picaud S. 2007. The toxicity of the PrP106-126 prion peptide on cultured photoreceptors correlates with the prion protein distribution in the mammalian and human retina. Am J Pathol 170:1314–1324. https://doi.org/10.2353/ajpath.2007.060340.

15. Head MW, Northcott V, Rennison K, Ritchie D, McCardle L, Bunn TJ, McLennan NF, Ironside JW, Tullo AB, Bonshek RE. 2003. Prion protein accumulation in eyes of patients with sporadic and variant Creutzfeldt-Jakob disease. Invest Ophthalmol Vis Sci 44:342–346. https://doi.org/10.1167/iovs.01-1273.

16. Parchi P, Strammiello R, Giese A, Kretzschmar H. 2011. Phenotypic variability of sporadic human prion disease and its molecular basis: past, present, and future. Acta Neuropathol 121:91–112. https://doi.org/10.1007/s00401-010-0779-6.

17. Ironside JW, Ritchie DL, Head MW. 2005. Phenotypic variability in human prion diseases. Neuropathol Appl Neurobiol 31:565–579. https://doi.org/10.1111/j.1365-2990.2005.00697.x.

18. Head MW, Bunn TJ, Bishop MT, McLoughlin V, Lowrie S, McKimmie CS, Williams MC, McCardle L, MacKenzie J, Knight R, Will RG, Ironside JW. 2004. Prion protein heterogeneity in sporadic but not variant Creutzfeldt-Jakob disease: UK cases 1991–2002. Ann Neurol 55:851–859. https://doi.org/10.1002/ana.20127.

19. Wadsworth JDF, Joiner S, Hill AF, Campbell TA, Desbruslais M, Luthert PJ, Collinge J. 2001. Tissue distribution of protease resistant prion protein in variant CJD using a highly sensitive immuno-blotting assay. Lancet 358:171–180. https://doi.org/10.1016/S0140-6736(01)05403-4.

20. Paterson RW, Torres-Chae CC, Kuo AL, Ando T, Nguyen EA, Wong K, DeArmond SJ, Haman A, Garcia P, Johnson DY, Miller BL, Geschwind MD.

21. 2012. Differential diagnosis of Jakob-Creutzfeldt disease. Arch Neurol 69:1578–1582. https://doi.org/10.1001/2013.jamaneurol.79.

21. Geschwind MD. 2010. Rapidly progressive dementia: prion diseases and other rapid dementias. Continuum (Minneap Minn) 16:31–56. https://doi.org/10.1212/01.CON.0000368211.79211.4c.

22. Parchi P, Zou W, Wang W, Brown P, Capellari S, Ghetti B, Kopp N, Schulz-Schaeffer WJ, Kretzschmar HA, Head MW, Ironside JW, Gambetti P, Chen SG. 2000. Genetic influence on the structural variations of the abnormal prion protein. Proc Natl Acad Sci U S A 97:10168–10172. https://doi.org/10.1073/pnas.97.18.10168.

23. Parchi P, Giese A, Capellari S, Brown P, Schulz-Schaeffer W, Windl O, Zerr I, Budka H, Kopp N, Piccardo P, Poser S, Rojiani A, Streichemberger N, Julien J, Vital C, Ghetti B, Gambetti P, Kretzschmar H. 1999. Classification of sporadic Creutzfeldt-Jakob disease based on molecular and phenotypic analysis of 300 subjects. Ann Neurol 46:224–233. https://doi.org/10.1002/1531-8249(199908)46:2<224::AID-ANA12>3.0.CO;2-W.

24. Collins SJ, Sanchez-Juan P, Masters CL, Klug GM, van Duijn C, Poleggi A, Pocchiari M, Almonti S, Cuadrado-Corrales N, de Pedro-Cuesta J, Budka H, Gelpi E, Glatzel M, Tolnay M, Hewer E, Zerr I, Heinemann U, Kretzschmar HA, Jansen GH, Olsen E, Mitrova E, Alpérovitch A, Brandel J-P, Mackenzie J, Murray K, Will RG. 2006. Determinants of diagnostic investigation sensitivities across the clinical spectrum of sporadic Creutzfeldt-Jakob disease. Brain 129:2278–2287. https://doi.org/10.1093/brain/awl159.

25. Puoti G, Bizzi A, Forloni G, Safar JG, Tagliavini F, Gambetti P. 2012. Sporadic human prion diseases: molecular insights and diagnosis. Lancet Neurol 11:618–628. https://doi.org/10.1016/S1474-4422(12)70063-7.

26. Brown P, Gibbs CJ, Jr, Rodgers Johnson P, Asher DM, Sulima MP, Bacote A, Goldfarb LG, Gajdusek DC. 1994. Human spongiform encephalopathy: the National Institutes of Health series of 300 cases of experimentally transmitted disease. Ann Neurol 35:513–529. https://doi.org/10.1002/ana.410350504.

27. Rabinovici GD, Wang PN, Levin J, Cook L, Pravdin M, Davis J, DeArmond SJ, Barbaro NM, Martindale J, Miller BL, Geschwind MD. 2006. First symptom in sporadic Creutzfeldt-Jakob disease. Neurology 66:286–287. https://doi.org/10.1212/01.wnl.0000196440.00297.67.

28. Armstrong RA. 2006. Creutzfeldt-Jakob disease and vision. Clin Exp Optom 89:3–9. https://doi.org/10.1111/j.1444-0938.2006.00001.x.

29. Lueck CJ, McIlwaine GG, Zeidler M. 2000. Creutzfeldt-Jakob disease and the eye. II. Ophthalmic and neuro-ophthalmic features. Eye 14:291–301. https://doi.org/10.1038/eye.2000.76.

30. Katz BJ, Warner JE, Digre KB, Creel DJ. 2000. Selective loss of the electroretinogram B-wave in a patient with Creutzfeldt-Jakob disease. J Neuroophthalmol 20:116–118. https://doi.org/10.1097/00041327-200020020-00011.

31. de Seze J, Hache JC, Vermersch P, Arndt CF, Maurage CA, Pasquier F, Laplanche JL, Ruchoux MM, Leys D, Destee A, Petit H. 1998. Creutzfeldt-Jakob disease: neurophysiologic visual impairments. Neurology 51: 962–967. https://doi.org/10.1212/WNL.51.4.962.

32. Head MW, Peden AH, Yull HM, Ritchie DL, Bonshek RE, Tullo AB, Ironside JW. 2005. Abnormal prion protein in the retina of the most commonly occurring subtype of sporadic Creutzfeldt-Jakob disease. Br J Ophthalmol 89:1131–1133. https://doi.org/10.1136/bjo.2004.063495.

33. Armitage WJ, Tullo AB, Ironside JW. 2009. Risk of Creutzfeldt-Jakob disease transmission by ocular surgery and tissue transplantation. Eye (Lond) 23:1926–1930. https://doi.org/10.1038/eye.2008.381.

34. Lim R, Dhillon B, Kurian KM, Aspinall PA, Fernie K, Ironside JW. 2003. Retention of corneal epithelial cells following Goldmann tonometry: implications for CJD risk. Br J Ophthalmol 87:583–586. https://doi.org/10.1136/bjo.87.5.583.

35. Gain P, Jullienne R, He Z, Aldossary M, Acquart S, Cognasse F, Thuret G. 2016. Global survey of corneal transplantation and eye banking. JAMA Ophthalmol 134:167–173. https://doi.org/10.1001/jamaophthalmol.2015.4776.

36. Tateishi J. 1985. Transmission of Creutzfeldt-Jakob disease from human blood and urine into mice. Lancet ii:1074.

37. Duffy P, Wolf J, Collins G, DeVoe AG, Streeten B, Cowen D. 1974. Possible

person-to-person transmission of Creutzfeldt-Jakob disease. N Engl J Med 290:692–693.

38. Heckmann JG, Lang CJ, Petruch F, Druschky A, Erb C, Brown P, Neundorfer B. 1997. Transmission of Creutzfeldt-Jakob disease via a corneal transplant. J Neurol Neurosurg Psychiatry 63:388–390. https://doi.org/10.1136/jnnp.63.3.388.

39. Rabinstein AA, Whiteman ML, Shebert RT. 2002. Abnormal diffusion-weighted magnetic resonance imaging in Creutzfeldt-Jakob disease following corneal transplantations. Arch Neurol 59:637–639. https://doi.org/10.1001/archneur.59.4.637.

40. Hammersmith KM, Cohen EJ, Rapuano CJ, Laibson PR. 2004. Creutzfeldt-Jakob disease following corneal transplantation. Cornea 23:406–408. https://doi.org/10.1097/00003226-200405000-00019.

41. Uchiyama KIC, Yago S, Kurumaya H, Kitamoto T. 1994. An autopsy case of Creutzfeldt-Jakob disease associated with corneal transplantation. Dementia 8:466–473.

42. Bongianni M, Orru C, Groveman BR, Sacchetto L, Fiorini M, Tonoli G, Triva G, Capaldi S, Testi S, Ferrari S, Cagnin A, Ladogana A, Poleggi A, Colaizzo E, Tiple D, Vaianella L, Castriciano S, Marchioni D, Hughson AG, Imperiale D, Cattaruzza T, Fabrizi GM, Pocchiari M, Monaco S, Caughey B, Zanusso G. 2017. Diagnosis of human prion disease using real-time quaking-induced conversion testing of olfactory mucosa and cerebrospinal fluid samples. JAMA Neurol 74:155–162. https://doi.org/10.1001/jamaneurol.2016.4614.

43. Foutz A, Appleby B, Hamlin C, Liu X, Yang S, Cohen Y, Chen W, Blevins J, Fausett C, Wang H, Gambetti P, Zhang S, Hughson A, Tatsuoka C, Schonberger LB, Cohen ML, Caughey B, Safar JG. 2017. Diagnostic and prognostic value of human prion detection in cerebrospinal fluid. Ann Neurol 81:79–92. https://doi.org/10.1002/ana.24833.

44. Wilham JM, Orru CD, Bessen RA, Atarashi R, Sano K, Race B, Meade-White KD, Taubner LM, Timmes A, Caughey B. 2010. Rapid end-point quantitation of prion seeding activity with sensitivity comparable to bioassays. PLoS Pathog 6:e1001217. https://doi.org/10.1371/journal.ppat.1001217.

45. Atarashi R, Satoh K, Sano K, Fuse T, Yamaguchi N, Ishibashi D, Matsubara T, Nakagaki T, Yamanaka H, Shirabe S, Yamada M, Mizusawa H, Kitamoto T, Klug G, McGlade A, Collins SJ, Nishida N. 2011. Ultrasensitive human prion detection in cerebrospinal fluid by real-time quaking-induced conversion. Nat Med 17:175–178. https://doi.org/10.1038/nm.2294.

46. Herms J, Tings T, Gall S, Madlung A, Giese A, Siebert H, Schurmann P, Windl O, Brose N, Kretzschmar H. 1999. Evidence of presynaptic location and function of the prion protein. J Neurosci 19:8866–8875. https://doi.org/10.1523/JNEUROSCI.19-20-08866.1999.

47. Beekes M, McBride PA, Baldauf E. 1998. Cerebral targeting indicates vagal spread of infection in hamsters fed with scrapie. J Gen Virol 79:601–607. https://doi.org/10.1099/0022-1317-79-3-601.

48. McBride PA, Schulz-Schaeffer WJ, Donaldson M, Bruce M, Diringer H, Kretzschmar HA, Beekes M. 2001. Early spread of scrapie from the gastrointestinal tract to the central nervous system involves autonomic fibers of the splanchnic and vagus nerves. J Virol 75:9320–9327. https://doi.org/10.1128/JVI.75.19.9320-9327.2001.

49. Prinz M, Heikenwalder M, Junt T, Schwarz P, Glatzel M, Heppner FL, Fu YX, Lipp M, Aguzzi A. 2003. Positioning of follicular dendritic cells within the spleen controls prion neuroinvasion. Nature 425:957–962. https://doi.org/10.1038/nature02072.

50. Glatzel M, Heppner FL, Albers KM, Aguzzi A. 2001. Sympathetic innervation of lymphoreticular organs is rate limiting for prion neuroinvasion. Neuron 31:25–34. https://doi.org/10.1016/S0896-6273(01)00331-2.

51. West Greenlee MH, Lind M, Kokemuller R, Mammadova N, Kondru N, Manne S, Smith J, Kanthasamy A, Greenlee J. 2016. Temporal resolution of misfolded prion protein transport, accumulation, glial activation, and neuronal death in the retinas of mice inoculated with scrapie. Am J Pathol 186:2302–2309. https://doi.org/10.1016/j.ajpath.2016.05.018.

52. Reference deleted.

53. Reference deleted.

54. Brunette I, Roberts CJ, Vidal F, Harissi-Dagher M, Lachaine J, Sheardown H, Durr GM, Proulx S, Griffith M. 2017. Alternatives to eye bank native tissue for corneal stromal replacement. Prog Retin Eye Res 59:97–130. https://doi.org/10.1016/j.preteyeres.2017.04.002.

55. Chen Z, You J, Liu X, Cooper S, Hodge C, Sutton G, Crook JM, Wallace GG. 2018. Biomaterials for corneal bioengineering. Biomed Mater 13:032002. https://doi.org/10.1088/1748-605X/aa92d2.

56. Clavaguera F, Bolmont T, Crowther RA, Abramowski D, Frank S, Probst A, Fraser G, Stalder AK, Beibel M, Staufenbiel M, Jucker M, Goedert M, Tolnay M. 2009. Transmission and spreading of tauopathy in transgenic mouse brain. Nat Cell Biol 11:909–913. https://doi.org/10.1038/ncb1901.

57. Irwin DJ, Lee VM, Trojanowski JQ. 2013. Parkinson's disease dementia: convergence of alpha-synuclein, tau and amyloid-beta pathologies. Nat Rev Neurosci 14:626–636. https://doi.org/10.1038/nrn3549.

58. Luk KC, Kehm V, Carroll J, Zhang B, O'Brien P, Trojanowski JQ, Lee VM. 2012. Pathological alpha-synuclein transmission initiates Parkinson-like neurodegeneration in nontransgenic mice. Science 338:949–953. https://doi.org/10.1126/science.1227157.

59. Walker LC, Schelle J, Jucker M. 2016. The prion-like properties of amyloid-beta assemblies: implications for Alzheimer's disease. Cold Spring Harb Perspect Med 6:a024398. https://doi.org/10.1101/cshperspect.a024398.

60. Geschwind MD, Josephs KA, Parisi JE, Keegan BM. 2007. A 54-year-old man with slowness of movement and confusion. Neurology 69:1881–1887. https://doi.org/10.1212/01.wnl.0000290370.14036.69.

61. Staffaroni AM, Elahi FM, McDermott D, Marton K, Karageorgiou E, Sacco S, Paoletti M, Caverzasi E, Hess CP, Rosen HJ, Geschwind MD. 2017. Neuroimaging in dementia. Semin Neurol 37:510–537. https://doi.org/10.1055/s-0037-1608808.

62. Kong Q, Zheng M, Casalone C, Qing L, Huang S, Chakraborty B, Wang P, Chen F, Cali I, Corona C, Martucci F, Iulini B, Acutis P, Wang L, Liang J, Wang M, Li X, Monaco S, Zanusso G, Zou WQ, Caramelli M, Gambetti P. 2008. Evaluation of the human transmission risk of an atypical bovine spongiform encephalopathy prion strain. J Virol 82:3697–3701. https://doi.org/10.1128/JVI.02561-07.

63. Gibson RM, Meyer AM, Winner D, Archer J, Feyertag F, Ruiz-Mateos E, Leal M, Robertson DL, Schmotzer CL, Quiñones-Mateu ME. 2014. Sensitive deep-sequencing-based HIV-1 genotyping assay to simultaneously determine susceptibility to protease, reverse transcriptase, integrase, and maturation inhibitors, as well as HIV-1 coreceptor tropism. Antimicrob Agents Chemother 58:2167–2185. https://doi.org/10.1128/AAC.02710-13.

64. Schippling S, Balk LJ, Costello F, Albrecht P, Balcer L, Calabresi PA, Frederiksen JL, Frohman E, Green AJ, Klistorner A, Outteryck O, Paul F, Plant GT, Traber G, Vermersch P, Villoslada P, Wolf S, Petzold A. 2015. Quality control for retinal OCT in multiple sclerosis: validation of the OSCAR-IB criteria. Mult Scler 21:163–170. https://doi.org/10.1177/1352458514538110.

65. Tewarie P, Balk L, Costello F, Green A, Martin R, Schippling S, Petzold A. 2012. The OSCAR-IB consensus criteria for retinal OCT quality assessment. PLoS One 7:e34823. https://doi.org/10.1371/journal.pone.0034823.

66. Cruz-Herranz A, Balk LJ, Oberwahrenbrock T, Saidha S, Martinez-Lapiscina EH, Lagreze WA, Schuman JS, Villoslada P, Calabresi P, Balcer L, Petzold A, Green AJ, Paul F, Brandt AU, Albrecht P. 2016. The APOSTEL recommendations for reporting quantitative optical coherence tomography studies. Neurology 86:2303–2309. https://doi.org/10.1212/WNL.0000000000002774.

67. Polymenidou M, Moos R, Scott M, Sigurdson C, Shi YZ, Yajima B, Hafner-Bratkovic I, Jerala R, Hornemann S, Wüthrich K, Bellon A, Vey M, Garen G, James MN, Kav N, Aguzzi A. 2008. The POM monoclonals: a comprehensive set of antibodies to non-overlapping prion protein epitopes. PLoS One 3:e3872. https://doi.org/10.1371/journal.pone.0003872.

68. Dougherty RM. 1964. Animal virus titration techniques, p 183–186. In Harris RJC (ed), Techniques in experimental virology. Academic Press, Inc., New York, NY.